Quantum-Size Effects on the Pressure-Induced Direct-to-Indirect Band-Gap Transition in InP Quantum Dots

Huaxiang Fu and Alex Zunger
National Renewable Energy Laboratory, Golden, Colorado 80401
(Received 5 November 1997)

We predict that the difference in quantum confinement energies of Γ-like and X-like conduction states in a covalent quantum dot will cause the direct-to-indirect transition to occur at substantially lower pressure than in the bulk material. Furthermore, the first-order transition in the bulk is predicted to become, for certain dot sizes, a second-order transition. Measurements of the "anticrossing gap" could thus be used to obtain unique information on the Γ-X-L intervalley coupling, predicted here to be surprisingly large (50–100 meV). [S0031-9007(98)06301-7]

PACS numbers: 71.24.+q, 73.20.Dx

Reduced dimensions usually cause pressure-induced structural phase transitions to occur at *elevated* pressures relative to the bulk solid. This is the case for the AlAs layers in AlAs/GaAs superlattices [1], for the transition to β-Sn structure in Si nanocrystals [2], and for the wurzite-to-rocksalt structure in CdSe dots [3]. Here, we show that reduced dimensionality causes another type of pressure-induced transition—the electronic direct-to-indirect transition—to occur at *reduced* pressures relative to the bulk.

Pressure-induced direct (Γ_{1c}) to indirect (X_{1c}) transitions occur in *bulk* zinc blende semiconductors [4,5] because under pressure, the Γ_{1c} energy goes up while the X_{1c} energy goes down [Figs. 1(a) and 1(b)]. This reflects the fundamentally different charge distribution in these two states [6]: the antibonding Γ_{1c} state has a node along the cation-anion bond, so it is destabilized (moves up in energy) as this bond is shortened, while the X_{1c} state has most of its amplitude in the interstitial volume, where no atoms exist. As a result of the different signs of the Γ_{1c} and X_{1c} deformation potentials, in materials where at zero pressure the energy of the X_{1c} state is not too far above the Γ_{1c} state (GaAs[4], InP[5], but not InAs or CdSe), a pressure-induced first-order $\Gamma_{1c} \rightarrow X_{1c}$ level crossing [7] occurs before the material is structurally phase transformed.

Reduced dimensionality can alter the energetic separation between the Γ_{1c}-like and X_{1c}-like states even without pressure [Figs. 1(b) and 1(c)]. This results from the fact that quantum confinement raises the energy of Γ_{1c} (with lighter mass) faster than the energy of X_{1c} (with heavier mass) [Figs. 1(b) and 1(c)]. Thus, if the energy of the X_{1c} state is not too far above the Γ_{1c} state in bulk, reduced size alone can cause a direct-to-indirect transition to occur *at zero pressure*. Detailed calculations [8] without pressure effect predicted this to occur in GaAs films, wires, and dots as size diminishes. Because of the larger ($\sim$0.95 eV, measured [9]) $\Gamma_{1c} - X_{1c}$ separation in bulk InP relative to in bulk GaAs (0.55 eV [10]), no direct-to-indirect transition was predicted to occur in free-standing InP dots at zero pressure [11]. Since, however, quantum confinement in InP dots could reduce the $\Gamma_{1c} - X_{1c}$ energy separation relative to the bulk, it might take less pressure to transform the dot than to transform the bulk into an indirect band gap [Figs. 1(c)–1(d)]. This hypothesis is examined and verified here. We show that the predicted low-pressure direct-to-indirect transition opens the door to obtaining unique information on the Γ-X and L-X interband mixings in dots via measurements of their energy levels vs pressure. We predict surprisingly large Γ-X-L couplings in dots (50–100 meV), suggesting that one (effective-mass) or a few ($\mathbf{k} \cdot \mathbf{p}$) band models which neglect (or significantly restrict) such interactions may be inadequate for describing such systems.

We construct T_d-symmetric InP quantum dots by including in the model all atoms within a given radius. The dots are either P centered or In centered. All surface dangling bonds are passivated [11] by attaching to them fictitious atoms. The atomic arrays in the interior of the dot are assumed to be bulklike, which is a good approximation for passivated dots [11]. We then solve the single-particle Schrödinger equation

$$\left\{-\frac{1}{2}\nabla^2 + \sum_{n,\alpha} v_\alpha(\mathbf{r} - \mathbf{R}_n - \mathbf{d}_\alpha; \Omega)\right\}\psi_i = \epsilon_i(\Omega)\psi_i\,, \tag{1}$$

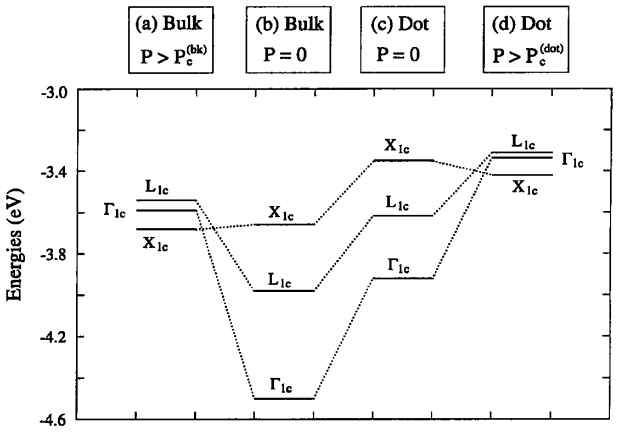

FIG. 1. Schematic illustration of the relative energy positions of Γ_{1c}, X_{1c}, and L_{1c} states of InP, showing how the Γ-X separation changes due to quantum size effect and pressure.

as a function of volume Ω. Here, $v_\alpha(\mathbf{r})$ is the screened, strain-dependent nonlocal pseudopotential of atom type α (e.g., In, P, or passivant) fitted [11] to the measured bulk band structure and effective masses, and to the calculated [via local density approximation (LDA)] deformation potentials and charge densities. Using our pseudopotentials the calculated *absolute* InP deformation potentials are -1.39, -7.73, $+0.88$, and -3.38 eV for Γ_{15v}, Γ_{1c}, X_{1c}, and L_{1c}, respectively, while the *ab initio* LAPW (linearized augmented plane wave) values [12] are -1.00, -6.26, $+0.65$, -3.30 eV, respectively. The measured [13,14] *relative* $\Gamma_{1c}-\Gamma_{15v}$ and $X_{1c}-\Gamma_{15v}$ deformation potentials are -6.40 and $+2.20$ eV, respectively, compared with our calculated values -6.34 and $+2.27$ eV, respectively. To solve Eq. (1) we expand $\{\psi_i\}$ in plane waves, and evaluate the matrix elements in this basis numerically. We diagonalize directly the Hamiltonian using the linear-size-scaling folded spectrum method [15]. We consider two experimentally accessible [2,3] dot sizes with diameters of 20.2 and 34.8 Å (175 and 891 atoms, respectively). Precisely the same method (i.e., pseudopotentials and basis set) is used to calculate the bulk band structure of InP, except that zinc blende periodic boundary conditions are applied.

Figure 2 shows the energies of the bulk InP Γ_{1c} and X_{1c} conduction states vs lattice constant a, exhibiting a crossing at $a = 5.5852$ Å; the deformation relative to the LDA calculated zero-pressure lattice constant (at which our pseudopotential is generated) is $\Delta a/a = 0.0414$. The measured [5] bulk $\Delta a/a = 0.0370$ corresponding to a transition pressure [5] of 112 kbar is within 10% (Table I [5,16]).

Figure 3 shows the energies of three lowest conduction states of P-centered InP dots vs lattice constant near the critical transition point. We see that unlike the bulk, where the $\Gamma \rightarrow X$ transition is first order (i.e., level crossing), the transition of the lowest conduction state in *dots* can be, depending on size, either first order (i.e., level crossing) or second order (i.e., level anticrossing). Table I shows the values of the deformations needed

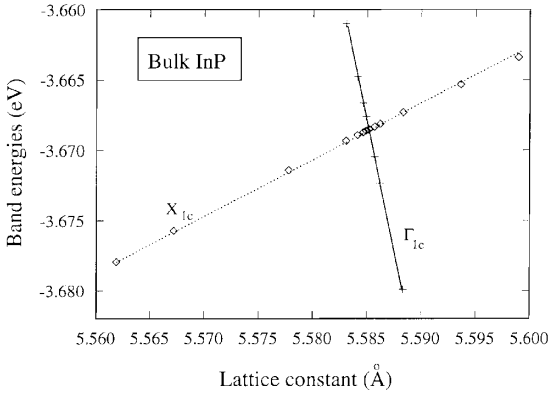

FIG. 2. Variations of the Γ_{1c} and X_{1c} band energies with lattice compression in bulk InP near the critical point.

TABLE I. Calculated and measured lattice constants a_{eq} (in Å) and relative deformations $\Delta a/a = (a_{\text{eq}} - a_{\text{tr}})/a_{\text{eq}}$ for direct-to-indirect transitions in bulk and in spherical quantum dots of InP. Wherever there are two rows in the table, the first row gives the values for level-crossing (C) transition, while the second row gives the values for level anticrossing (AC).

		P-centered InP dots	
Quantity	Bulk InP	$D = 34.8$ Å	$D = 20.2$ Å
a_{eq} (expt.)	5.8658[a]	...	...
a_{eq} (calc.)	5.8265	...	...
$a_{\Gamma\rightarrow X}$ (expt.)	5.6489[b]	...	...
$a_{\Gamma\rightarrow X}$ (calc.)	5.5852	5.6862[c](C)	5.6511
		5.6838(AC)	5.6600[c]
$\Delta a/a$ (expt.)	0.0370	...	...
$\Delta a/a$ (calc.)	0.0414	0.0241[c](C)	0.0301
		0.0245(AC)	0.0286[c]

[a]Ref. [16], [b]Ref. [5], [c]The transition which occurs at lower pressure.

to obtain the direct-to-indirect transition in quantum dots: for the $D = 34.8$ Å dot, the critical deformation is predicted to be reduced to $\sim 60\%$ of the bulk value. Experimental testings of this prediction of quantum-size induced reduction in the critical pressure are needed.

The reduction of the critical pressure in dots is caused mostly by the reduction of zero-pressure $X_{1c}-\Gamma_{1c}$ energy separation in dot relative to in bulk. To estimate this effect we note that at zero pressure ($\Omega = \Omega_{\text{eq}}$) and for $D = 34.8$ Å dot, our calculated confinement energies $\Delta\epsilon_\gamma(\Omega) = \epsilon_\gamma^{\text{dot}}(\Omega) - \epsilon_\gamma^{\text{bulk}}(\Omega)$ for the lowest $\gamma = X_{1c}$-like ($\gamma = \Gamma_{1c}$-like) conduction states are 0.31 (0.58) eV.

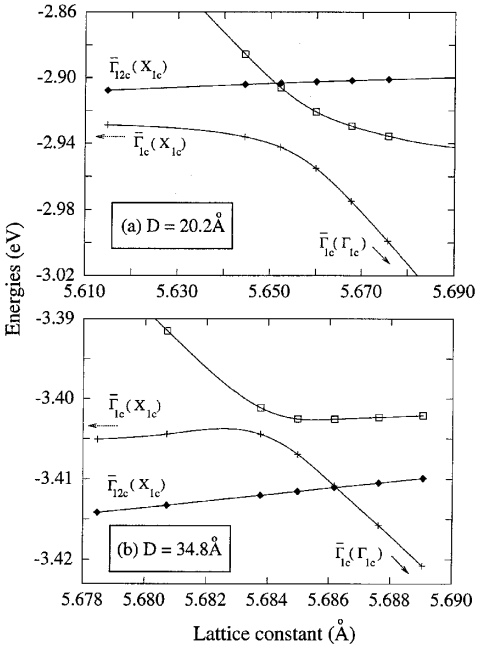

FIG. 3. Variations of the three lowest conduction states $\bar{\Gamma}_{1c}(\Gamma_{1c})$, $\bar{\Gamma}_{1c}(X_{1c})$, and $\bar{\Gamma}_{12c}(X_{1c})$ in P-centered InP dots with lattice compression near the critical point: (a) $D = 20.2$ Å dot; (b) $D = 34.8$ Å dot.

Thus, the X_{1c}-Γ_{1c} energy difference is reduced in this dot by 0.27 eV relative to the bulk value.

Interestingly, (i) the confinement energies $\Delta\epsilon_\gamma(\Omega)$ are nearly pressure independent. They are 0.28 (0.60) eV at the transition volume $\Omega = 0.93\Omega_{\rm eq}$, and 0.31 (0.58) eV at $\Omega_{\rm eq}$ for the X_{1c} (Γ_{1c}) state of the $D = 34.8$ Å dot. This suggests that the reduced size affects the dot's wave function *macroscopically* (i.e., by altering the envelope part), while the pressure affects the wave function *microscopically* (by changing the periodic Bloch part). The fact that the confinement energies are close for the zero-pressure dot and for the compressed dot, provides one way to obtain the quantum size effect on those states at Brillouin-zone edge, which proved to be difficult under ambient pressure [17]. (ii) The X_{1c} confinement energy obtained in our direct diagonalization approach [Eq. (1)] is surprisingly *larger* than what was expected from effective-mass approximation (EMA): using the calculated effective masses [11] $m_e^*(\Gamma_{1c}) = 0.095$, $m_e^*(X_{1c}) = 2.04$, the EMA gives 0.06 (1.31) eV for the confinement energy of X_{1c}-like (Γ_{1c}-like) conduction state. Thus, the EMA predicts that the $\Gamma \rightarrow X$ transition will already occur at zero pressure for this $D = 34.8$ Å dot. Actually, we find that an accurate description of the *whole* lowest bulk conduction band (not just near Γ and X as in the EMA) is needed to predict the correct Γ-X energy separation (thus the critical pressure) in dots. (iii) Our calculations further show that the reduction of Γ-X energy separation relative to the bulk value is not a simple monotonic function of dot size (the reduction is 0.15, 0.27, and 0.00 eV for $D = 20.2$, 34.8, and ∞ Å dots, respectively). (iv) One interesting issue regarding InP dots is the envelope-function symmetry of the top valence state. We find that the envelope is s-like both at zero pressure and near the transition pressure. This is consistent with point (i) that the pressure does not change the property due to envelope difference.

To understand the level crossings and anticrossings evident in Fig. 3 we consider the symmetries of the states of the bulk and the dots (Table II). In the diamondlike bulk band structure, the lowest X conduction state is twofold degenerate (neglecting spin), while in zinc-blende band structure, it is broken into two singly degenerate states X_{1c} and X_{3c}. In both cases, there are three equivalent X valleys. In zinc blende, if the origin of the coordinate system is placed at the anion site [18], the lowest X conduction state (e.g., in InP or GaP) is found [19] to be X_{1c} (s symmetry at the anion, p symmetry at the cation), while the next lowest X conduction state (about 0.4 eV higher in bulk InP) is X_{3c} (s symmetry at the cation, p symmetry at the anion). When the *anion* is perturbed (e.g., P-centered dots), the new states (marked with an overbar) relate to the parent zinc-blende states (shown in parentheses) as indicated in Table II: X_{1c}-derived states yield the $\overline{\Gamma}_{1c} + \overline{\Gamma}_{12c}$ states (singly and doubly degenerate, respectively), while X_{3c}-derived states yield the $\overline{\Gamma}_{15c}$ states (triply degenerate). The original zinc-blende Γ_{1c} state retains its $\overline{\Gamma}_{1c}$ symmetry. For the *cation* site perturbation (e.g., In-centered dots), the roles of X_{1c} and X_{3c} are exchanged (Table II). Now, states of the same symmetry must repel each other (anticross) in response to a symmetry-preserving perturbation. This is the case for $\overline{\Gamma}_{1c}(\Gamma_{1c})$ and $\overline{\Gamma}_{1c}(X_{1c})$. In contrast, states with different symmetries can cross. This is the case for $\overline{\Gamma}_{1c}(\Gamma_{1c})$ and $\overline{\Gamma}_{12c}(X_{1c})$. The symmetry considerations explain the behavior seen in Fig. 3. Figure 3(b) and Table I show that in the larger dot (34.8 Å), crossing occurs first, at $\Delta a/a = 0.0241$, while anticrossing occurs at a slightly larger deformation $\Delta a/a = 0.0245$. The order of these events can change with size [see Fig. 3(a)].

The "anticrossing gap" (the smallest energy difference between repelling curves in Fig. 3) measures the effective Γ-X coupling (i.e., $2V_{\Gamma X}$). We find $2V_{\Gamma X} = 0$ for

TABLE II. Symmetries of the Γ-like, X-like, and L-like conduction states in bulk InP and in InP dots with different atoms at the dot center. Overbar denotes the state in the dot while its bulk parentage is given in parentheses.

Bulk states	Anion-centered	Cation-centered
Γ_{1c}	$\overline{\Gamma}_{1c}(\Gamma_{1c})$	$\overline{\Gamma}_{1c}(\Gamma_{1c})$
X_{1c}	$\overline{\Gamma}_{1c}(X_{1c}) + \overline{\Gamma}_{12c}(X_{1c})$	$\overline{\Gamma}_{15c}(X_{1c})$
X_{3c}	$\overline{\Gamma}_{15c}(X_{3c})$	$\overline{\Gamma}_{1c}(X_{3c}) + \overline{\Gamma}_{12c}(X_{3c})$
L_{1c}	$\overline{\Gamma}_{1c}(L_{1c}) + \overline{\Gamma}_{15c}(L_{1c})$	$\overline{\Gamma}_{1c}(L_{1c}) + \overline{\Gamma}_{15c}(L_{1c})$
Γ_{15c}	$\overline{\Gamma}_{15c}(\Gamma_{15c})$	$\overline{\Gamma}_{15c}(\Gamma_{15c})$

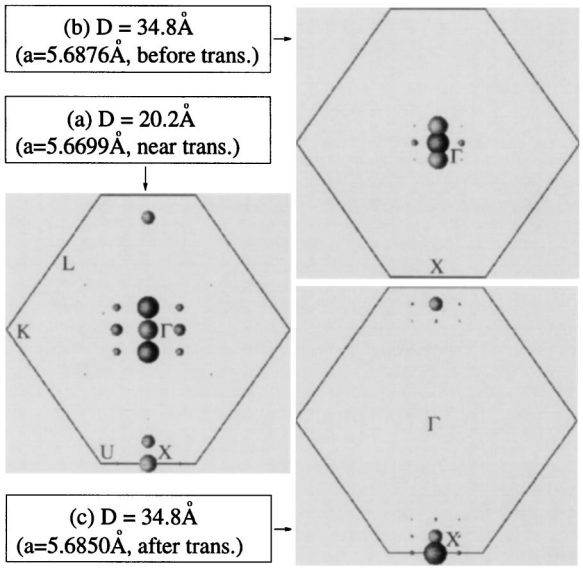

FIG. 4. Spectral decomposition of the lowest conduction wave functions of the following P-centered dots onto those bulk states with wave vector **k** in the plane passing Γ, L, K, U, X points of zinc blende Brillouin zone: (a) $D = 20.2$ Å dot at the anticrossing transition; (b) $D = 34.8$ Å dot before the transition; (c) $D = 34.8$ Å dot after the transition. The larger the sphere size, the larger the contribution from this bulk state.

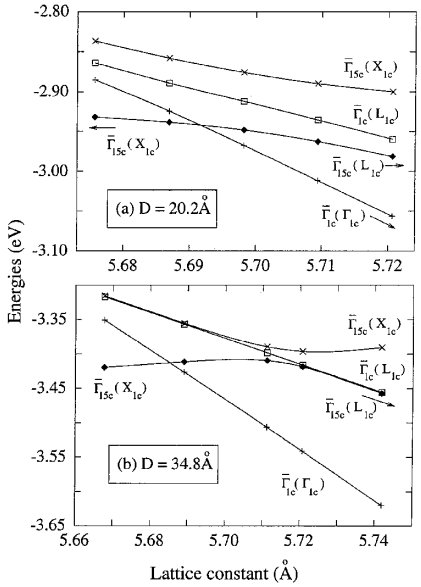

FIG. 5. Variation of the near-edge conduction states $\overline{\Gamma}_{1c}(\Gamma_{1c})$, $\overline{\Gamma}_{1c}(L_{1c})$, $\overline{\Gamma}_{15c}(L_{1c})$, and $\overline{\Gamma}_{15c}(X_{1c})$ of In-centered InP dots with lattice compression near the critical point: (a) $D = 20.2$ Å dot; (b) $D = 34.8$ Å dot.

bulk, 3.3 meV for $D = 34.8$ Å dot, and 34.2 meV for $D = 20.2$ Å dot. The size scaling of Γ-X coupling is $V_{\Gamma X} \sim 1/D^{\lambda}$ with $\lambda = 4.30$. This shows that reduction in quantum size enhances dramatically interstate coupling. Our Γ-X coupling values are much larger than the values predicted [20] and measured [21] in AlAs/GaAs and InAs/GaAs nanostructures, respectively, where the Γ and X states are *spatially separated* in different materials. The large anticrossing gap predicted here for InP dot [Fig. 3(a)] implies that the direct-to-indirect transition will be smeared over a range of pressures, as the states there are neither pure Γ nor pure X. This can be seen in the projection of the dot wave function $\psi_i(\mathbf{r})$ onto the zinc-blende Bloch states (Fig. 4): while for the larger dot the states before (after) the transition are almost pure Γ (X); for the smaller dot, no such sharp distinction exists.

Figure 5 shows the energies vs lattice constant for the In-centered dots. The relative transition deformation $\Delta a/a$ is 0.0232 (0.0243) for a smaller (larger) In-centered dot. The lowest X-like conduction state $\overline{\Gamma}_{15c}(X_{1c})$ first anticrosses with the L-like conduction state $\overline{\Gamma}_{15c}(L_{1c})$ and then, as the pressure is increased, it crosses with the Γ-like conduction state $\overline{\Gamma}_{1c}(\Gamma_{1c})$. The coupling strength between $\overline{\Gamma}_{15c}(X_{1c})$ and $\overline{\Gamma}_{15c}(L_{1c})$ is $2V_{LX} = 71.6$ (10.2) meV for the smaller (larger) dot considered. Thus, the L-X coupling is *significantly* larger than the Γ-X coupling for the dot of the same size. Note that the difference in ΓX coupling between In- and P-centered dots reflects the wave function (rather than the dot surface) difference on the atomic scale. If the dots are neither In nor P centered, the difference between Figs. 3 and 5 may be obscured, and a perturbation from the two representative cases considered here may occur.

In summary, we study the interplay between quantum size and pressure effects in InP dots. We find that the quantum confinement energy is nearly independent of the pressure. We predict the $\Gamma \rightarrow X$ transitions in InP dots to occur at finite pressure (unlike GaAs [8]), but significantly below the bulk value. The unexpectedly large confinement energy for an X-like state is important in describing the Γ-X transition. Such Γ-X transitions can be used to reveal the extent of interband coupling in dots. We predict Γ-X coupling of 34.2 (3.3) meV and L-X coupling of 71.6 (10.2) meV for $D = 20.2$ Å ($D = 34.8$ Å) dots.

We thank S. H. Wei and L. W. Wang for fruitful discussions. This work was supported by the U.S. Department of Energy, OER-BES, under Grant No. DE-AC36-83CH10093.

[1] B. A. Weinstein *et al.*, Phys. Rev. Lett. **58**, 781 (1987).
[2] S. H. Tolbert *et al.*, Phys. Rev. Lett. **76**, 4384 (1996).
[3] S. H. Tolbert and A. P. Alivisatos, Science **265**, 373 (1994).
[4] D. J. Wolford and J. A. Bradley, Solid State Commun. **53**, 1069 (1985).
[5] S. Ernst, A. R. Goni, K. Syassen, and M. Cardona, Phys. Rev. B **53**, 1287 (1996).
[6] D. M. Wood, A. Zunger, and R. de Groot, Phys. Rev. B **31**, 2570 (1985).
[7] P. E. Van Camp, V. E. Van Doren, and J. T. Devresse, Phys. Rev. B **41**, 1598 (1990).
[8] A. Franceschetti and A. Zunger, Phys. Rev. B **52**, 14 664 (1995); Appl. Phys. Lett. **68**, 3455 (1996).
[9] J. Camassel, P. Merle, L. Bayo, and H. Mathieu, Phys. Rev. B **22**, 2020 (1980).
[10] T. C. Chiang, J. A. Knapp, M. Aano, and D. E. Eastman, Phys. Rev. B **21**, 3513 (1980).
[11] H. Fu and A. Zunger, Phys. Rev. B **56**, 1496 (1997); **55**, 1642 (1997). These papers describe the zero strain case. For the strain case, the atomic potentials are $v = v_{\mathrm{eq}}(1 + \beta \frac{a-a_{\mathrm{eq}}}{a_{\mathrm{eq}}})$ with $\beta = 1.125$ (1.072) for In (P) atom.
[12] S.-H. Wei and A. Zunger (unpublished).
[13] H. Müller, R. Trommer, M. Cardona, and P. Vogl, Phys. Rev. B **21**, 4879 (1980).
[14] C. S. Menoni and I. L. Spain, Phys. Rev. B **35**, 7520 (1987).
[15] L. W. Wang and A. Zunger, J. Chem. Phys. **100**, 2394 (1994).
[16] P. Deus *et al.*, Phys. Status. Solidi A **103**, 443 (1987).
[17] M. Ben-Chorin *et al.*, Phys. Rev. Lett. **77**, 763 (1996).
[18] T. N. Morgan, Phys. Rev. Lett. **21**, 819 (1968).
[19] S. H. Wei and A. Zunger, J. Appl. Phys. **63**, 5794 (1988).
[20] L. W. Wang, A. Franceschetti, and A. Zunger, Phys. Rev. Lett. **78**, 2819 (1997).
[21] G. H. Li, A. R. Goni, K. Syassen, O. Brandt, and K. Ploog, Phys. Rev. B **50**, 18 420 (1994).